Binding of Cationic (+4) Alanine- and Glycine-Containing Oligopeptides to Double-Stranded DNA: Thermodynamic Analysis of Effects of Coulombic Interactions and α-Helix Induction†

S. Padmanabhan,‡,§,|| Wentao Zhang,‡,§ Michael W. Capp,§ Charles F. Anderson,§ and M. Thomas Record, Jr.*,§,⊥

Departments of Chemistry and Biochemistry, University of Wisconsin−Madison, Madison, Wisconsin 53706

Received November 27, 1996; Revised Manuscript Received February 14, 1997⊗

ABSTRACT: Coulombic interactions and coupled conformational changes make important contributions to stability and specificity of many protein−nucleic acid complexes. As models of these phenomena in simpler systems, we have investigated the binding to mononucleosomal (160 base-pair) calf thymus DNA of a high charge density (compact) 5-residue (+4) oligopeptide (with 4 lysines and 1 tryptophan) and of four lower charge density (extended) 17-residue (+4) oligopeptides (each with 4 lysines, 10−12 alanines, 0−2 glycines, and 1 tryptophan). The fractional helicity (f_h) of each oligopeptide before and after DNA binding was determined using circular dichroism. At low univalent cation concentration ($[M^+] = 6.4$ mM), binding to DNA increases f_h significantly for all but one of the extended oligopeptides. Oligopeptide−DNA binding constants (K_{obs}) and apparent binding site sizes (n) were quantified using the noncooperative McGhee−von Hippel isotherm to fit tryptophan fluorescence quenching data. For each of the oligopeptides studied, n is found to be approximately equal to four, the number of lysine charges. In the range 6.4 mM $\leq [M^+] \leq$ 21.5 mM, power dependences of K_{obs} on $[M^+]$ ($SK_{obs} \equiv$ d log K_{obs}/d log$[M^+]$) for all 17-residue (+4) oligopeptides are similar with an average value of -3.7 ± 0.4, which is indistinguishable (outside uncertainty) from the value obtained here for the compact (+4) oligopeptide and from values reported elsewhere for another compact tetralysine and for spermine (+4). Our results are consistent with the conclusion that the nonspecific binding to DNA of all these tetravalent ligands is driven primarily by coulombic interactions. At any $[M^+]$ investigated, values of K_{obs} for the four extended (+4) oligopeptides differ by less than an order of magnitude, but all are 1−2 orders of magnitude less than values of K_{obs} for two compact (+4) oligopeptides and for spermine. The differences in K_{obs} for oligopeptide−DNA complexes, which all have similar n and similar SK_{obs}, indicate that when an extended oligopeptide binds to DNA it becomes more compact as a result of conformational changes, such as the additional α-helix formation detected by circular dichroism.

Binding of proteins to DNA is driven in large part by the favorable thermodynamic consequences of reducing DNA polyanionic charge density (polyelectrolyte effect) and of burying nonpolar surface (hydrophobic effect) [see Record et al. (1991) and Spolar and Record (1994)]. Local protein folding transitions and other conformational changes, driven by binding free energy, create functionally important parts of the specific protein−DNA interface and give rise to a characteristic thermodynamic signature (Spolar & Record, 1994). In particular, α-helix formation is coupled to specific binding of many gene regulatory proteins and of oligopeptides corresponding to the DNA-binding regions of various proteins (Arrowsmith et al., 1990; O'Neill et al., 1990, 1991; Talanian et al., 1990; Zhang et al., 1994; Lewis et al., 1996) and restriction enzymes (McClarin et al., 1986; Jen-Jacobson et al., 1986; Newman et al., 1995). For proteins that interact nonspecifically with DNA, smaller increases in helicity induced by binding have been reported (Arrowsmith et al., 1990; O'Neill et al., 1990, 1991; Zhang et al., 1994; Percipalle et al., 1995). Johnson et al. (1994) demonstrated that increases in α-helicity of low charge density (extended) lysine-containing alanine oligopeptides [as determined by circular dichroism (CD)[1]] occur upon nonspecific binding to duplex DNA oligonucleotides. High charge density (compact) lysine oligopeptides (with net charge z ranging from 3 to 10 positive charges) have been used as model systems in investigations of salt concentration effects on the thermodynamics of protein−DNA interactions (Latt & Sober, 1967a,b; Lohman et al., 1980; Mascotti & Lohman, 1990, 1992, 1993; Zhang et al., 1996). For compact and extended DNA-binding oligopeptides, more systematic and quantitative comparisons should provide better understanding of how oligopeptide charge, structure, and helix-forming propensity affect the thermodynamic parameters that characterize their nonspecific binding to DNA.

In the present study, we characterize and compare the nonspecific binding to double-helical 160 base-pair (bp) mononucleosomal calf thymus DNA (CT DNA) of five oligopeptides, specified in Table 1. These model (+4) ligands, one compact (5-residue) and four extended (17-

† This research was supported by NIH Grant GM 34351.

* Corresponding author.
‡ The first two authors contributed equally to this study.
§ Department of Chemistry.
|| Present address: Instituto de Estructura de la Materia "Rocasolano", CSIC, 119 Serrano, 28020 Madrid, Spain.
⊥ Department of Biochemistry.

⊗ Abstract published in *Advance ACS Abstracts,* April 15, 1997.

[1] Abbreviations: CD, circular dichroism; bp, base pair; CT DNA, mononucleosomal calf thymus DNA (160 bp); ds, double-stranded; [DNAP], DNA phosphate (monomer) concentration.

S0006-2960(96)02927-3 CCC: $14.00

Table 1: Cationic Oligopeptides (L^{4+})

oligopeptide	sequence	K−K spacing
	Extended 17-Residue AK Oligopeptides	
AK1	Ac-W-K-AAA-K-AAAA-K-AAA-K-AA-amide	(*i*,*i*+4; *i*,*i*+5; *i*,*i*+4)
AK2	Ac-W-K-AAAA-K-AAAA-K-AAAA-K-amide	(*i*,*i*+5)
	Extended 17-Residue AKG Oligopeptides	
AKG1	Ac-W-K-AAA-K-A-GG-A-K-AAA-K-AA-amide	(*i*,*i*+4; *i*,*i*+5; *i*,*i*+4)
AKG2	Ac-W-K-AAAA-K-A-GG-A-K-AAAA-K-amide	(*i*,*i*+5)
	Compact 5-Residue Oligopeptide	
WK_4	Ac-W-KKKK-amide	
	Compact 4-Residue Oligopeptide[a]	
KWK_2	K-W-KK-amide	

[a] Investigated by Mascotti and Lohman (1993).

residue), exhibit a range of flexibility and fractional helicity in the unbound state. All have four positively charged lysines (at neutral pH), an amide (uncharged) at the C-terminus, and an acetylated (uncharged) N-terminal tryptophan, which is used for fluorescence and absorbance detection. The coulombic contribution to the DNA binding of the (+4) oligopeptides studied here should be directly comparable with that of other (+4) oligocations including spermine (Braunlin et al., 1982) and the lysine oligopeptide KWK_2 (Mascotti & Lohman, 1993).

For alanine oligopeptides, extensive information is available on the thermodynamics of α-helix formation, on the helix-forming propensities of various guest amino acids, and on the side-chain interactions that affect helix stability (Baldwin, 1995, and references therein). The two 17-residue alanine−lysine (AK) oligopeptides studied here were chosen to exhibit moderate α-helix propensities in aqueous solution. In the two 17-residue AKG oligopeptides studied here, two centrally-located alanine residues were replaced with helix-destabilizing glycines to produce more flexible conformations with lower average α-helix propensities than the corresponding AK oligopeptides. With only five residues, WK_4 is considerably more compact than either AK or AKG and is expected to be nonhelical because of its short length (5 residues) and relatively high charge density.

The oligopeptides AKG2 and AK2 have lysines in identical positions in the sequence, separated by four residues (*i*,*i*+5). Separations between lysines in AKG1 and AK1 also are identical: (*i*,*i*+4) between K2 and K6 and between K11 and K15, and (*i*,*i*+5) between K6 and K11. Helix-destabilizing coulombic repulsions are greater for lysines with spacing (*i*,*i*+4) because this spacing corresponds most closely to one α-helical turn. Consequently, at low salt concentrations, where charge-screening is relatively ineffective, AK1 is expected to be less helical than AK2. Increases in salt concentration reduce the effects of coulombic repulsions among lysine charges and hence increase the fractional helicity of AK1 in solution (Baldwin, 1995) as does binding to DNA (Johnson et al., 1994).

The oligopeptides studied in this paper should be useful models for sites on proteins that undergo coupled folding transitions upon binding to DNA, because they exhibit differences in the distribution of ligand charges and in the propensity to form α-helical structure. By analyzing binding data at various salt concentrations using the McGhee−von Hippel (1974) isotherm, we quantify and compare: binding site sizes (n); nonspecific site binding constants (K_{obs}) as well as the corresponding binding free energies ($\Delta G^{\circ}_{obs} \equiv -RT \ln K_{obs}$); $[M^+]$-dependences of K_{obs} ($SK_{obs} \equiv d \log K_{obs}/d \log [M^+]$); and values of $\Delta\mu_L^{conf}$, the contribution to ΔG°_{obs} due to the change in the conformation of the oligopeptide occurring when it binds to DNA. The extent to which any conformational change of a bound oligopeptide can be attributed to an increase in helicity is investigated by analyzing the change in its CD spectrum upon binding using a modification of the Lifson and Roig (1961) theory (Doig et al., 1994).

MATERIALS AND METHODS

Preparation, Purification, and Characterization of Oligopeptides. The oligopeptides listed in Table 1 were synthesized by the solid-phase method using the simultaneous multiple peptide synthesis procedure (Houghten, 1985; Houghten et al., 1986). Each synthesis of a C-terminal amidated oligopeptide was performed in a separate fine mesh polypropylene bag [Propyltex fabric (74 μm), Tetko Inc. Chicago, IL] on a 0.03−0.05 mmol scale using 0.1−0.15 g of a 0.3 milliequiv/g of PAL (polystyrene Fmoc, 9-fluorenylmethoxycarbonyl) resin (Milligen). The active ester coupling procedure using the pentafluorophenyl (OPfp) esters of the Fmoc amino acids (Milligen) was used in the synthesis. The N-termini of the oligopeptides were acetylated using acetic anhydride and cleaved from the resin as oligopeptide amides using a 95:5 (vol:vol) trifluoroacetic acid (TFA): anisole mixture. The crude oligopeptides then were purified using a semipreparative C18 reverse-phase column (Beckman Ultrasphere 5 μm resin in 25 cm × 1 cm column or a Kromasil 100 Å, 5 μm C18 reverse-phase column) with water−acetonitrile (0.1% TFA) gradients run at a flow rate of 1.5 mL/min and monitored at 225 nm. The eluted oligopeptides then were lyophilized to yield approximately 99% purity. Amino acid identities were confirmed by matrix-assisted laser desorption ionization mass spectrometry (Department of Chemistry, University of Wisconsin−Madison). Prior to spectroscopic measurements, fresh stock solutions (∼0.5 mM) were prepared by dissolving the lyophilized oligopeptide in water, and the oligopeptide concentration was determined from the absorbance of the N-terminal tryptophan at 280 nm in 6 M guanidinium hydrochloride using $\epsilon_{280} = 5690\ M^{-1}\ cm^{-1}$ (Edelhoch, 1967). This N-terminal tryptophan also serves as a means of monitoring oligopeptide−DNA binding by tryptophan fluorescence quenching.

The pK_a of the lysine ϵ-NH_2 in alanine−lysine oligopeptides is approximately 11.5 in 10 mM NaCl at 0 °C

(Marqusee & Baldwin, 1987). We conclude that, over the range of concentrations and solution conditions employed in the present study, the free oligopeptides did not aggregate because the tryptophan fluorescence intensity is linear with oligopeptide concentration (data not shown); the circular dichroism signal is independent of oligopeptide concentration (Baldwin, 1995, and references therein); and K_{obs} is independent of changes in oligopeptide and DNA concentrations, as indicated by our titrations with DNA at different oligopeptide concentrations. [However, a 17-residue +4 oligopeptide in which all lysines are phased (*i*,*i*+4) is observed to gel at moderate concentrations (J. Ballin, personal communication).] On the basis of the reversibility of DNA binding, the reproducibility of the maximum fluorescence quenching, the reversible temperature dependence of the CD signal induced by DNA-binding, and the results of light scattering experiments (data not shown), we conclude that no aggregation occurs in the solutions containing both oligopeptide and DNA under the conditions investigated.

Preparation of Native Mononucleosomal Calf Thymus DNA. The 160 ± 5 bp mononucleosomal CT DNA was purified from calf thymus glands as described by Wang et al. (1990). Its size was verified by gel electrophoresis in a 7.5% polyacrylamide gel using a pBR322 size marker obtained from an *Hpa*II and *Eco*R1 restriction digest. All the DNA samples exhibited ratios of the UV absorbances at 260 nm and 280 nm larger than 1.82, as expected for a protein-free preparation. To remove excess NaCl and any multivalent metal ion impurities, stock solutions of the 160 bp CT DNA (DNA phosphate concentration, [DNAP] ≳ 10 mM) were extensively dialyzed (in tubing with ~10^4 g/mol cutoff) at 4 °C to yield a ratio $[Na^+]/[DNAP]$ of ~1:1 (Stein et al., 1995). Values of [DNAP] were determined from its absorbance at 260 nm in a Cary 210 spectrophotometer using an extinction coefficient, $\epsilon = 6410\ M^{-1}\ cm^{-1}$, calculated from nearest neighbor frequencies (Allen et al., 1972; Stein et al., 1995). The hyperchromicity upon alkaline denaturation at 260 nm was ~30%, indicating that the DNA was double-stranded (before and after oligopeptide binding).

Circular Dichroism Measurements. CD measurements were performed on an Aviv 60DS spectropolarimeter equipped with a Hewlett-Packard 89100A temperature control unit (Department of Biochemistry, Stanford University). The spectropolarimeter was calibrated with (+)-10-camphorsulfonic acid (Chen & Yang, 1977). CD spectra of oligopeptide, DNA, and oligopeptide−DNA solutions, obtained in K_2HPO_4 buffer (pH 7.0, 6.4 mM K^+) at 5 and 25 °C using a 1 mm path length cuvette and 0.2 nm step size, were averaged over four scans. The oligopeptide concentration was typically 20 μM. To ensure complete binding of all oligopeptides to DNA, oligopeptide−DNA spectra were obtained in a 16-fold excess [DNAP] (~315 μM) and a relatively low $[K^+] = 6.4$ mM. The CD spectrum of each oligopeptide−DNA complex was obtained by subtracting the CD spectrum of the corresponding DNA−buffer solution from the CD spectrum of the oligopeptide−DNA−buffer solution. Mean molar residue ellipticities at 222 nm, $[\theta]_{222}$ (in deg cm^2 $dmol^{-1}$), were measured in 10 mm path length cuvettes for oligopeptide concentrations of approximately 20 μM at pH 7.0 at the specified temperature (5−43 °C) and K^+ concentration (6.4 mM and 1.0 M, where $[K^+]$ was increased with KCl). (The DNA remains native at all temperatures investigated.) Measurements in 10% trifluoroethanol (TFE) at 5 °C, 0.1 M KCl, pH 7.0, were performed as described by Nelson and Kallenbach (1986).

Determination and Analysis of Fractional Helicity. Experimental values of f_h, the fractional helicity, were determined from $[\theta]_{222}$ measurements using a baseline value (in the absence of aromatic residues) of $[\theta]_{222,0\%} = +640$ for 0% helix and $[\theta]_{222,100\%} = -40\,000\,[1 - (2.5/N_r)]$ for 100% helix, where $N_r = 17$, the number of amino acid residues (Scholtz et al., 1991a). Chakrabartty et al. (1993) showed that the aromatic tryptophan side chain contributes −2300 ± 600 deg cm^2 $dmol^{-1}$ ($[\theta]^{100\%}_{222,w}$) to the CD signal at 222 nm when tryptophan is in a nearly 100% helical oligopeptide (at 1 M salt) and makes no significant contribution when the tryptophan is nonhelical. In a subsequent paper, Chakrabartty et al. (1994) assumed a simple proportionality between the tryptophan contribution and f_h of the oligopeptide. We calculate f_h from CD signals using their expression.

$$f_h = ([\theta]_{222} - [\theta]_{222,0\%})/([\theta]_{222,100\%} - [\theta]_{222,0\%} + [\theta]^{100\%}_{222,w}) \quad (1)$$

Values of f_h calculated with eq 1 were analyzed using a modified form of the Lifson−Roig theory (1961) of helix−coil transitions (Doig et al., 1994), as outlined in the Appendix. This model (here designated MLR) is formulated with the following sequence-independent relative statistical weights: "*w*" related to helix propagation; "v" related to helix nucleation; and "n_{cap}" and "c_{cap}" were deduced experimentally from N- and C-terminal capping effects. In the present application of the MLR model, a minimal number of conformational parameters suffices to characterize the thermodynamic coupling of helix induction with DNA binding. Therefore, for a given oligopeptide the same average value of *w* is assigned to every type of residue (but the different extended oligopeptides are characterized by different average values of *w*). The binding of an oligopeptide to DNA is assumed to cause a change in *w*, but not in any of the other statistical weights (v, n_{cap}, or c_{cap}), which were assigned values reported for similar alanine oligopeptides (Doig & Baldwin, 1995). [For the tryptophan residue, c_{cap} is assigned a value of unity in the absence of experimental data (Doig & Baldwin, 1995).]

Fluorescence Titrations. Oligopeptide binding to DNA was monitored by tryptophan fluorescence quenching in an SLM-Aminco 8000C spectrofluorometer (Urbana, IL) using an excitation wavelength of 296 nm and an emission wavelength of 350 nm in order to minimize absorbance by DNA and inner filter corrections (Mascotti & Lohman, 1992). Solutions of oligopeptides (3−10 μM initial concentration) and DNA (0.5−2.0 mM DNAP) for fluorescence titrations were prepared from stocks diluted to identical salt and buffer concentrations. The binding buffer (pH 7.0) was made up of 0.2 mM Na_2EDTA, 1 mM NaH_2PO_4, 1 mM $Na_2B_4O_7$, and 1 mM trisodium citrate (for a total $[Na^+] = 6.4$ mM). At the low salt concentrations of these binding experiments, the use of different cations (Na^+ vs K^+) and different buffer anions for the fluorescence and CD measurements is not expected to be of any significance. Interchanging these two cations produces no change in the salt concentration dependence of K_{obs} for binding of oligocationic ligands to DNA (Mascotti & Lohman, 1990). At the (relatively low) salt concentrations investigated here no specific effects of the

buffer anions on conformational or binding equilibria of oligopeptides or nucleic acids have been reported.

At least two different concentrations of each oligopeptide were titrated with DNA in the presence of a fixed concentration of excess Na^+. The fluorescence quenching data for these "reverse" titrations were corrected for dilution and inner filter effects, as described by Lohman and Mascotti (1992), using $\epsilon_{296} = 1700(\pm100)$ M^{-1} cm^{-1} for the N-terminal tryptophan and $\epsilon_{296} = 570(\pm30)$ M^{-1} cm^{-1} for CT DNA. All titrations were performed in a siliconized quartz cuvette to minimize ligand (i.e., oligopeptide) adsorption to the cuvette walls. The temperature was regulated by a circulating constant-temperature Neslab RTE-220 water bath. Photobleaching was minimized by use of minimal excitation slit widths (2 or 3 nm) and by opening the excitation shutter only during the fluorescence intensity measurement. Photobleaching was negligible under these conditions; after an hour of continuous irradiation, the fluorescence signal decreased by less than 2%. The fluorescence intensity measured in oligopeptide−DNA titrations was corrected for background emission and Raman light scattering from water by subtracting corresponding signals measured during an equivalent titration of the buffer solution.

The extent of tryptophan fluorescence quenching (Q_{obs}) is defined as

$$Q_{obs} \equiv |F_{obs} - F_{init}|/F_{init} \quad (2)$$

where F_{obs} is the observed fluorescence intensity and F_{init} is the initial fluorescence intensity of the free oligopeptide. All fluorescence intensities were corrected for background fluorescence, dilution, and inner filter contributions (Lohman & Mascotti, 1992; Zhang et al., 1996). (The magnitude of the inner filter correction is proportional to the DNA concentration and is approximately 7%−15% of the observed fluorescence signal at approximately 0.1−0.3 mM DNAP.) Tryptophan fluorescence of these oligopeptides in the absence of DNA increases by no more than 3%−4% when $[M^+]$ is increased from 6 mM to 0.3 M (while significant increases in helicity occur over the same $[M^+]$ range) and hence is relatively insensitive to changes in coulombic interactions and/or in oligopeptide conformation, including increases in helicity caused by increased $[M^+]$. Therefore, observed changes in fluorescence quenching, as a function of ligand or DNA concentration at different fixed salt concentrations, can be attributed to changes in the extent of ligand binding without complications from changes in the tryptophan fluorescence in either the bound or free state of the oligopeptide. We estimate that the corrections to the fluorescence data described above, together with the usual random sources of error, produce experimental uncertainties that are approximately 10% when $[M^+] = 6.4$ mM and [DNAP] is relatively low and 15%−20% when $[M^+] = 21.5$ mM and [DNAP] is relatively high.

Salt concentration dependences of oligopeptide−DNA binding were determined from reverse titration data obtained at four different fixed salt concentrations, obtained by adding NaCl to the binding buffer (6.4 mM Na^+) to final $[Na^+]$ of 11.4, 16.5, and 21.5 mM, respectively. "Salt back-titrations", in which salt is added to displace the ligand from DNA at fixed total concentrations of each of these reactants, were used only to assess the reversibility of the binding. The observation that approximately 90% of the fluorescence signal is recovered upon titration to high salt concentrations (>0.2 M; data not shown) indicates that binding is reversible.

Determination and Analysis of the Oligopeptide−DNA Binding Isotherm. The equilibrium binding "constant" for oligopeptide−DNA binding is defined (according to the usual convention) in terms of the equilibrium molar concentrations of reactants and product: $K_{obs} \equiv [LD]/[L][D]$. Here LD, L, and D designate the oligopeptide−DNA complex, free oligopeptide, and an isolated unoccupied binding site on DNA, respectively. To determine K_{obs} in the limit of low ligand binding density, reverse titration data (of excess L with D) were fitted using the McGhee−von Hippel (1974) binding isotherm:

$$K_{obs} = \frac{1}{[L]} \frac{\nu}{1 - n\nu} \left(\frac{1 - (n-1)\nu}{1 - n\nu} \right)^{n-1} \quad (3)$$

This expression was derived for non-cooperative binding of linear ligands of arbitrary length to a linear, homogeneous, infinite lattice with overlapping binding sites. Here n is the overlap-site size of the ligand (the number of potential ligand binding sites eliminated by one isolated bound ligand), and ν is the ligand binding density (the average fractional occupancy of a site). First by McGhee and von Hippel (1974) and subsequently by numerous other laboratories [see, for example, Record et al. (1976), Braunlin et al. (1982), Plum and Bloomfield (1988), and Mascotti and Lohman (1992)], eq 3 has been shown to describe the functional form of binding isotherms for the nonspecific interactions with DNA of a variety of oligocations, including oligopeptides. Because any anticooperativity has in effect been subsumed into n, this parameter generally is not integral. No dependence of n on ν, [L], or the concentration of excess salt (which fixes the magnitude of K_{obs}) has been observed here or in previous studies.

In our applications of eq 3 to fluorescence quenching data, $\nu = (Q_{obs}/Q_{max})([L_T]/[D_T])$ and $[L] = (1 - Q_{obs}/Q_{max})[L_T]$, respectively. Here $[D_T]$ and $[L_T]$ are the total concentrations of DNA sites and oligopeptide, respectively, Q_{obs} is defined in eq 2, and Q_{max} is the maximum fluorescence quenching (Mascotti & Lohman, 1992; Zhang et al., 1996). The 160 bp DNA is effectively infinite, insofar as the number of binding sites is not significantly fewer than the number of DNA phosphates.

The nonlinear least squares program NONLIN (Johnson & Frasier, 1985) was used to fit eq 3 to the fluorescence quenching data obtained in reverse titrations of L with D. The parameters K_{obs}, Q_{max}, and n were floated or fixed, as indicated in the tables and figure captions. The analysis assumes that Q_{obs} is directly proportional to $[L_B]/[L_T]$ (where L_B and L_T specify the bound and total oligopeptide, respectively). This assumption was verified previously by a ligand binding density analysis for tryptophan-containing oligolysines binding to DNA (Mascotti & Lohman, 1992; Zhang et al., 1996), and in the present study was verified for the binding of AKG2 to DNA (data not shown). For the tightest-binding oligopeptides (AK1, WK_4) values of n also were estimated from the intersection of the initial tangent line and the horizontal line at saturation in plots of Q_{obs} versus $[DNAP]/[L_T]$.

With values of K_{obs} determined from reverse titrations at various fixed salt concentrations, the dependence of K_{obs} on

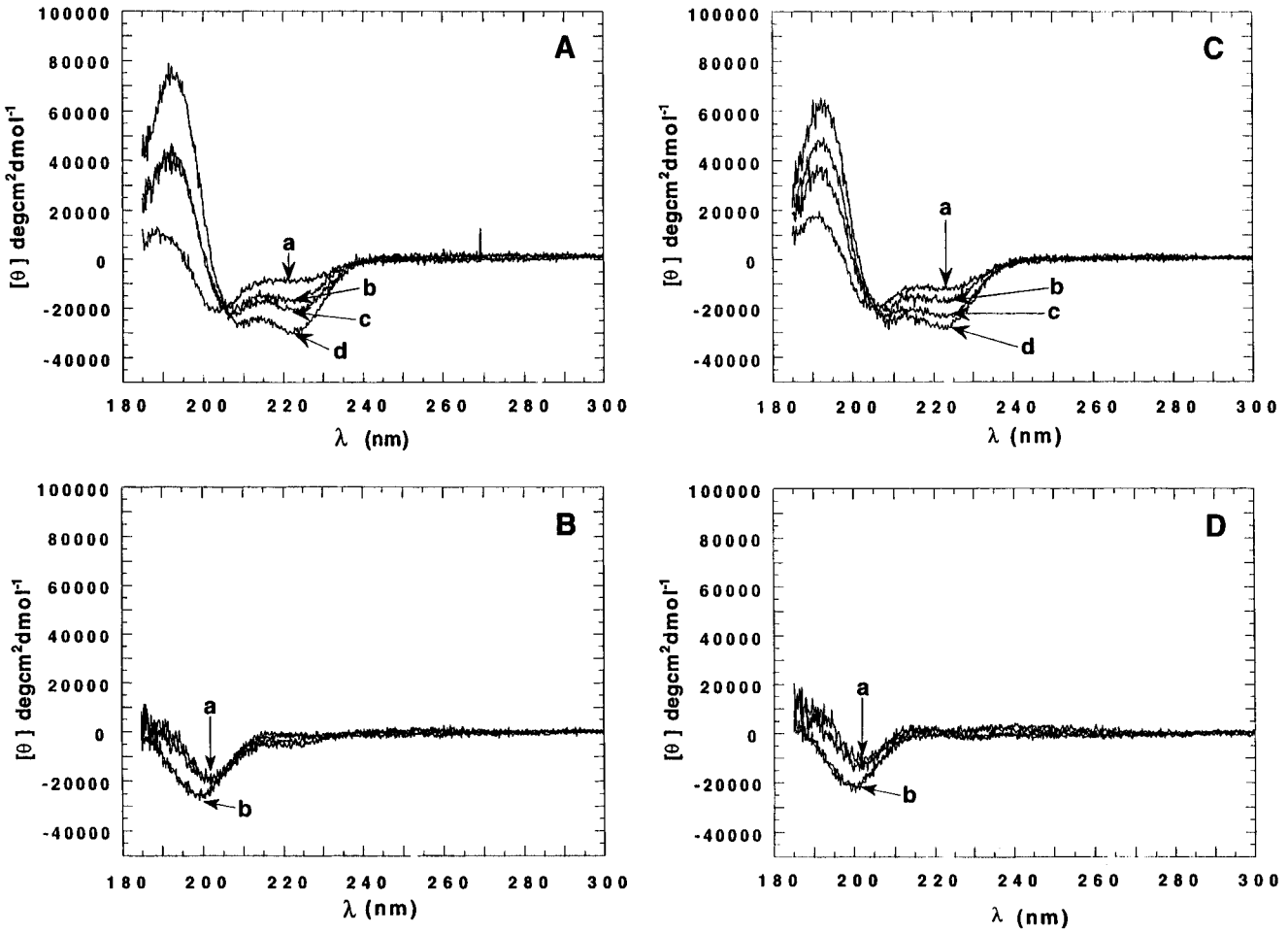

FIGURE 1: Circular dichroism spectra obtained in the absence and presence of CT DNA ([DNAP] = 315 μM), pH 7.0 (3.2 mM K_2HPO_4/6.4 mM K^+), [oligopeptide] $\approx$ 20 μM, at 5 or 25 °C. The mean molar residue ellipticities [θ] are plotted as a function of the wavelength (nm). (A) AK1: a, 25 °C, −DNA; b, 25 °C, +DNA; c, 5 °C, −DNA; d, 5 °C, +DNA. (B) AKG1: a, 5 or 25 °C, −DNA; b, 5 or 25 °C, +DNA. (C) AK2: a, 25 °C, −DNA; b, 25 °C, +DNA; c, 5 °C, −DNA; d, 5 °C, +DNA. (D) AKG2: a, 5, 25 °C, −DNA; b, 5, 25 °C, +DNA.

[M^+] was evaluated as the derivative $SK_{obs} \equiv$ d log K_{obs}/d log[M^+]. Over the range of [M^+] investigated here, the salt dependence of K_{obs} for 160 bp DNA is expected to exhibit minimal coulombic end effects (Olmsted et al., 1989, 1995; Stein et al., 1995). In the experiments used to evaluate K_{obs}, [M^+] was always in large excess over the concentrations of L, D and LD, but low enough (6.4−21.5 mM) so that experimentally determined values of SK_{obs} are only ~5% less negative than the corresponding calculated values of $S_a K_{obs} \equiv$ d log K_{obs}/d log $a_\pm$, where $a_\pm$ is the mean ionic activity of the univalent salt. This derivative is directly related to the preferential interaction coefficients that characterize the interactions of excess salt with each of the participants in the binding interaction (Anderson & Record, 1993; Record & Anderson, 1995).

Table 2: Mean Molar Residue Ellipticities ($[\theta]_{222}$) of AK and AKG Oligopeptides

solution conditions[a]	$-[\theta]_{222}$(degcm²dmol⁻¹)[b] AK1	AKG1	AK2	AKG2
6.4 mM M^+, 5 °C				
free (−DNA)	20400	1000	24000	1600
bound (+DNA)	29000	6700	31400	1200
6.4 mM M^+, 25 °C				
free (−DNA)	8200	1000	12300	1000
bound (+DNA)	16900	3300	19400	1000
1.0 M M^+, 5 °C				
free (−DNA)	29000	3400	31500	4100
0.1 M M^+, 10 mol % TFE, 5 °C				
free (−DNA)	35500	19900	nd[c]	21500

[a] pH 7.0. [b] Error in the measurement of $-[\theta]_{222}$ is ≤3%. Amino acid sequences shown in Table 1. [c] nd, not determined.

EXPERIMENTAL AND COMPUTATIONAL RESULTS

Circular Dichroism Measurements of Oligopeptide and Oligopeptide−DNA Complexes. CD spectra of the 17-residue oligopeptides (AK1, AKG1, AK2, and AKG2) in the presence and absence of DNA at 5 and 25 °C are shown in Figures 1A−D. Spectra in the presence of DNA are difference spectra (explained in Materials and Methods), obtained at low (but excess) [M^+] and excess DNA ([DNAP]/[ligand] $\approx$ 16) to ensure complete (>99%) binding of the oligopeptide ligands. Table 2 lists values for $-[\theta]_{222}$ under the conditions indicated.

The CD spectra of AK1 and AK2 in solutions with and without DNA at 5 and 25 °C (Figures 1A and 1C, respectively) have two minima (one at 222 nm and the other between 205 and 210 nm), a maximum at approximately 190 nm, and an isodichroic point near 203 nm, consistent with the two-state model for each residue: helical or unstructured (Holzwarth & Doty, 1965). The presence of a minimum between 200 and 205 nm and the absences of a minimum at

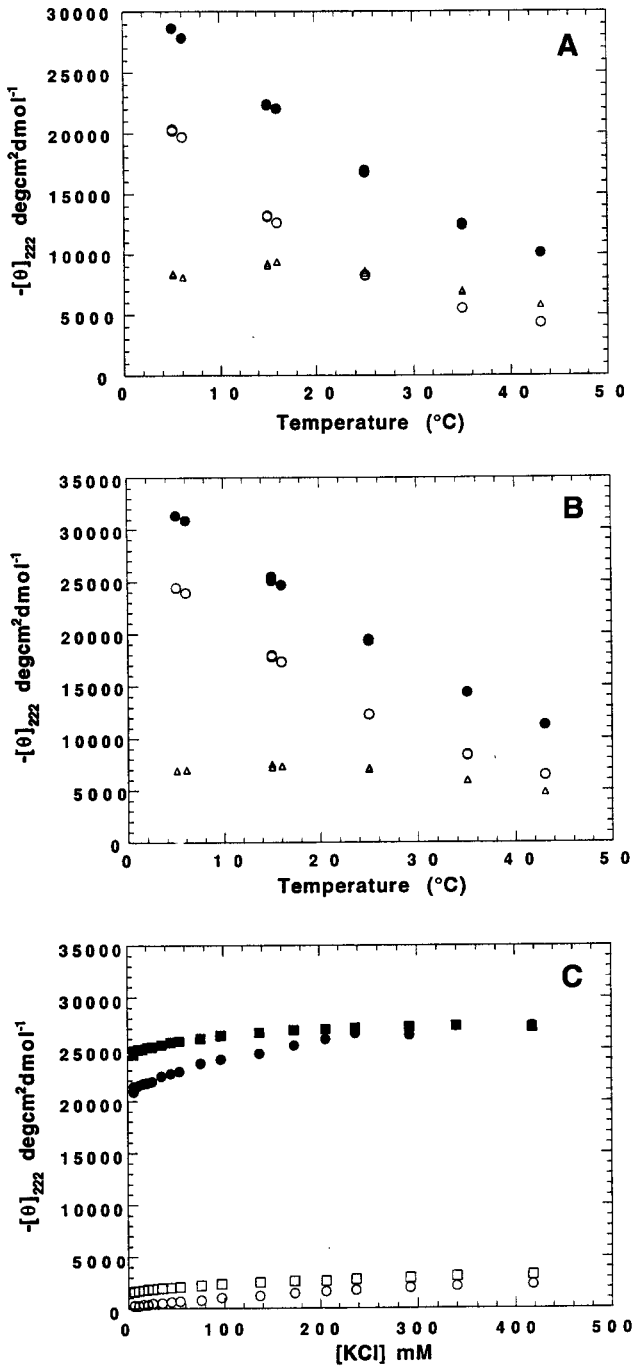

FIGURE 2: (A) Dependence of the mean molar residue ellipticities at 222 nm, ($[\theta]_{222}$ in deg cm^2 dmol^{-1}) on temperature for AK1 in the absence and in the presence of DNA. (B) Dependence of $[\theta]_{222}$ on temperature for AK2 in the absence and in the presence of DNA. In both A and B, solution conditions are [oligopeptide] $\approx$ 20 μM, [DNAP] = 315 μM, [K$^+$] = 6.4 mM, pH 7.0. Symbols represent oligopeptide (○), oligopeptide+DNA (●), and the difference between oligopeptide+DNA and oligopeptide (△). (C) Dependences of $[\theta]_{222}$ on salt concentration in the absence of DNA for AK1 (●), AKG1 (○), AK2 (■), and AKG2 (□) at 5 °C, pH 7.0, [oligopeptide] $\approx$ 20 μM.

222 nm and of a maximum near 190 nm in the CD spectra of AKG1 and AKG2, both with two central glycines, indicate negligible helicity at low [M$^+$] in the absence of DNA (Figures 1B and 1D, respectively). Under these conditions, for AK1 and AK2, formation of α-helical regions is intramolecular, as shown by their reversible, concentration-independent thermal unfolding monitored by our CD measurements (Figures 2A and 2B), in agreement with previous results (Scholtz et al., 1991b). Sedimentation equilibrium measurements also have demonstrated that helix formation is intramolecular in similar alanine oligopeptides (Padmanabhan et al., 1990).

The CD spectra of CT DNA in 6.4 mM M$^+$ at 5 and 25 °C are superimposable and characteristic of B-form DNA, with two maxima at 272 and 221 nm and a minimum at 248 nm (Chan et al., 1990). The CD signal at 222 nm remains unchanged between 0 and 43 °C. Furthermore, signal intensities between 260 and 300 nm (attributable to base stacking; Chan et al., 1990) are virtually identical in the presence and absence of each of the oligopeptides. Hence, their binding has no apparent effect on the DNA conformation, and so the changes in CD signal intensities in the far-UV region (200−240 nm) observed in oligopeptide−DNA solutions can be attributed exclusively to changes in the fractional helicity of the oligopeptide induced when it binds to DNA. This inference is in accord with extensive studies of specific and nonspecific binding of oligopeptides to DNA (O'Neil et al., 1990, 1991; Talanian et al., 1990; Johnson et al., 1994), which obtained no evidence of any DNA conformational change upon oligopeptide binding.

At two widely different [M$^+$] (6.4 mM and 1 M M$^+$) in the absence of DNA, f_h is negligible for the two oligopeptides having central glycines (AKG1, AKG2). At both high and low [M$^+$] the fractional helicity of free AK1 is less than that of free AK2, as expected from the smaller lysine spacing of AK1. For each of the oligopeptides, the increase in $-[\theta]_{222}$ with increasing salt concentration (Figure 2C) is consistent with previous results (Scholtz et al., 1991c). In 10% TFE, a helix-stabilizing mixed solvent, $-[\theta]_{222}$ for AK1 approaches the value expected for a 100% helical 17-residue oligopeptide (cf. Materials and Methods), whereas values of $-[\theta]_{222}$ for AKG1 and AKG2 are significantly lower, presumably because the two central glycines strongly favor less structured conformations.

In the presence of excess DNA at low [M$^+$] (6.4 mM M$^+$), the fractional helicities of AK1, AK2, and AKG1, but not AKG2, increase significantly over values observed in the absence of DNA. Under these conditions, where all of the oligopeptide is bound to DNA, values of $-[\theta]_{222}$ are either the same (AK1, AK2), somewhat larger (AKG1) or smaller (AKG2) than values in excess DNA at 1 M salt (Table 2). This binding produces a detectable shift in the equilibrium of helical and nonhelical residues of the bound oligopeptides (except for AKG2) but does not cause them to become completely helical, as indicated by the CD spectra of the bound oligopeptides (Figure 1).

Determinations of Average Helix Propensities (w) and Oligopeptide Conformational Partition Functions (Z^{MLR}). The formation of α-helical structure in short oligopeptides in aqueous solution is a moderately cooperative thermodynamic process (Scholtz et al., 1991a) which appears to be described adequately by statistical models, such as the modified form of the Lifson−Roig model (Doig et al., 1994) outlined in the Appendix. This model also should be applicable to describe the physical situation of interest here, where binding to DNA does not induce the entire oligopeptide to form an α-helix but does produce an increase in its overall average fractional helicity. For AK and AKG oligopeptides that are either bound (B) to DNA or free (F) in solution, Table 3 lists values of the residue-averaged helical propensities (w_B

Table 3: Average Helix Propagation Equilibrium Constants (w) and Modified Lifson−Roig Partition Functions (Z^{MLR}) Calculated from f_h for Extended Oligopeptides and Their DNA Complexes

oligopeptide	T (°C)	free ligand[a]			DNA complex[a]			$\Delta\mu_L^{MLR}$ [d] (kcal/mol)
		$f_{h,F}$[b]	Z_F^{MLR} [c]	w_F [c]	$f_{h,B}$[b]	Z_B^{MLR} [c]	w_B [c]	
AK1	5	56	11 ± 1	1.26 ± 0.01	79	62 ± 22	1.49 ± 0.04	1.0 ± 0.2
	25	24	4.2 ± 0.1	1.07 ± 0.01	47	8.0 ± 0.4	1.21 ± 0.01	0.4 ± 0.1
AK2	5	66	19 ± 2	1.33 ± 0.02	86	243 ± 237	1.66 ± 0.10	1.4 ± 0.6
	25	35	5.5 ± 0.2	1.14 ± 0.01	54	10 ± 1	1.25 ± 0.01	0.4 ± 0.1
AKG1	5	4.4	2.8 ± 0.1	0.78 ± 0.01	20	4.2 ± 0.1	1.03 ± 0.01	0.2 ± 0.1
	25	4.4	2.8 ± 0.1	0.78 ± 0.01	11	3.3 ± 0.1	0.93 ± 0.01	0.1 ± 0.1
AKG2	5	6.0	2.9 ± 0.1	0.83 ± 0.01	5.0	2.8 ± 0.1	0.80 ± 0.01	−0.0 ± 0.1
	25	4.4	2.8 ± 0.1	0.78 ± 0.01	4.4	2.8 ± 0.1	0.78 ± 0.01	0.0 ± 0.1

[a] Free (−DNA): 6.4 mM M^+, pH 7.0. Bound (+DNA): 6.4 mM M^+, 315 μM DNAP, pH = 7.0. [b] $f_{h,F}$ and $f_{h,B}$, fractional helicities for the free and bound oligopeptides, respectively, were calculated from the mean residue ellipticities ($-[\theta]_{222}$) listed in Table 2, as described in Materials and Methods. [c] Z_F^{MLR}, w_F: 6.4 mM M^+, no DNA. Z_B^{MLR}, w_B: 6.4 mM M^+, 315 μM DNAP. Errors in Z^{MLR} and w are estimated on the basis of the average 3% error in the CD determinations of $[\theta]_{222}$. [d] Calculated with eq 4. Errors are estimated from uncertainties in Z^{MLR}.

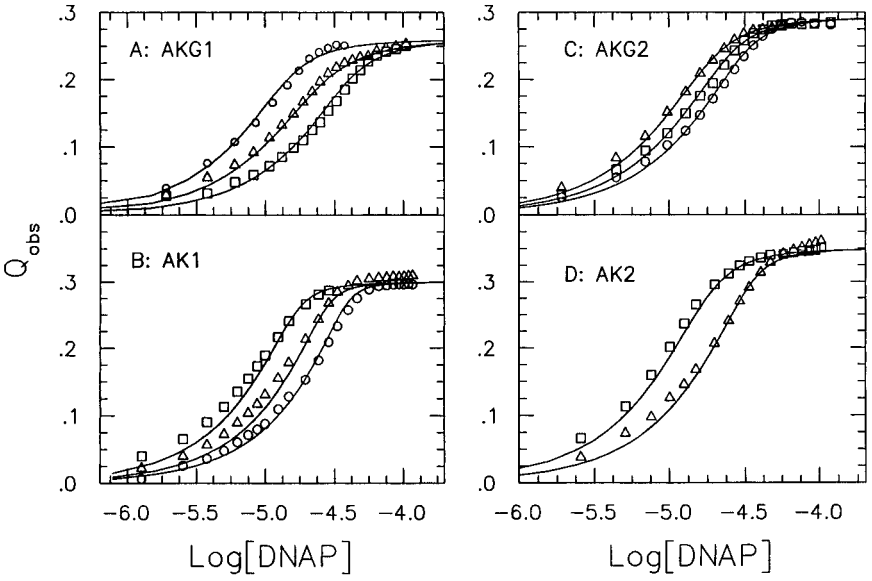

FIGURE 3: Representative reverse titrations of extended 17-residue (+4) oligopeptides with CT DNA in 6.4 mM Na^+, pH 7.0, 25 °C. The observed fluorescence quenching (cf eq 2) is plotted vs the logarithm of the molar concentration of DNA phosphates (monomer) added. (A) AKG1, initial concentrations of 2.23 (○), 3.18 (△), and 6.36 μM (□). (B) AK1, initial concentrations of 3.1 (□), 5.4 (△), and 7.7 μM (○). (C) AKG2, initial concentrations of 2.95 (△), 4.02 (□), and 5.36 μM (○). (D) AK2, initial concentrations of 3.1 (□) and 6.2 μM (△). Solid lines are the best global fittings of the McGhee−von Hippel isotherm (eq 3) to the reverse titration data for where n is fixed at its average value of ∼4 (cf. Table 4).

and w_F) and of the oligopeptide conformational partition functions (Z_B^{MLR} and Z_F^{MLR}) calculated under the specified conditions by analyzing CD data with the modified Lifson−Roig (MLR) model, as explained in the Appendix. Between 0 and 43 °C each of the w values decreases with increasing temperature, as indicated by the less negative values of $[\theta]_{222}$ shown in Figures 2A and 2B. This observation is consistent with lower helix stability at higher temperature, and with the finding that helix denaturation in water is generally endothermic (Scholtz et al., 1991b). At all temperatures investigated here the best-fit values of w_B and Z_B^{MLR} for AK1 and AK2 at low salt ($[M^+]$ = 6.4 mM) in the presence of DNA are greater than the corresponding values of w_F and Z_F^{MLR} obtained at the same $[M^+]$ in the absence of DNA. (According to eq A2, Z^{MLR} increases monotonically with w.)

Also given in Table 3 are values of $\Delta\mu_L^{MLR}$, the (theoretical) change in the chemical potential of each of the extended oligopeptides that is due to a change in helicity (as monitored by f_h) of the ligand when it binds to DNA. The tabulated values of were calculated (according to the modified Lifson−Roig model described in the Appendix) with the expression

$$\Delta\mu_L^{MLR} = RT \ln(Z_B^{MLR}/Z_F^{MLR}) \quad (4)$$

The resulting values of $\Delta\mu_L^{MLR}$ fall in the range 0.4−1.3 kcal/mol and are larger at 5 than at 25 °C. The calculations of $\Delta\mu_L^{MLR}$ presented in Table 3 indicate that binding to DNA stabilizes additional α-helical structure of AK1, AK2, and AKG1. For the binding of each of the extended oligopeptides to DNA, $\Delta\mu_L^{MLR}$ and other contributions to ΔG°_{obs} are considered in more detail at the end of the Results.

Tryptophan Fluorescence Quenching Measurements of Oligopeptide−DNA Binding Parameters. Figures 3A−D report the results of representative reverse titrations of AKG1, AK1, AKG2, and AK2 (2−8 μM), respectively, with CT DNA in 6.4 mM M^+, pH 7.0, and 25 °C. The tryptophan fluorescence quenching, Q_{obs}, is plotted versus the logarithm of the DNA phosphate concentration, log[DNAP]. These data were analyzed by global fittings, in which the McGhee−von Hippel isotherm (eq 3) is fitted to all reverse titration data obtained at a given salt concentration for a given oligopeptide at different initial concentrations. These global fittings yield the best-fit values of the parameters listed in

Table 4: Parameters for Oligopeptide−DNA Binding from Fluorescence Titrations

oligopeptide	Q_{max}[a]	n[b]	log K_{obs} (M^{-1})[c]
AK1	0.30 ± 0.01	3.4 ± 0.2	6.00 ± 0.18
AKG1	0.26 ± 0.01	5.0 ± 0.4	5.89 ± 0.12
AK2	0.35 ± 0.01	3.5 ± 0.2	5.80 ± 0.13
AKG2	0.29 ± 0.01	3.9 ± 0.2	5.76 ± 0.10
WK_4	0.31 ± 0.01	4.6 ± 0.5	7.84 ± 1.36

[a] Maximum fluorescence quenching. [b] McGhee−von Hippel (1974) site size evaluated as best-fit parameter using eq 3. [c] McGhee−von Hippel (1974) binding constants at pH 7.0, 6.4 mM M^+, 25 °C evaluated as best-fit parameter using eq 3 (n floated).

Table 5: Salt Concentration Dependences of Oligocation (L^{4+}) DNA Interactions

oligocation (L^{4+})	SK_{obs}[a]	log K_{obs} (1 M M^+)[b]	log K_{obs} (6.4 mM M^+)[c]
AK1[c]	−4.0 ± 0.1	−2.36 ± 0.24	6.43 ± 0.12
AKG1[c]	−3.4 ± 0.5	−1.61 ± 0.81	5.63 ± 0.10
AK2[c]	−3.4 ±0.4	−1.59 ± 0.77	5.84 ± 0.15
AKG2[c]	−3.3 ± 0.1	−1.73 ± 0.34	5.82 ± 0.04
WK_4[c]	−4.1 ± 0.3	−1.91 ± 0.60	6.90 ± 0.26
KWK_2[d]	−3.5 ± 0.3	−0.34 ± 0.32	7.43 ± 0.73 [f]
spermine[e]	−3.3 ± 0.3	0.20 ± 0.20	7.44 ± 0.69 [f]

[a] $SK_{obs} \equiv$ d log K_{obs}/d log[M^+]. [b] Extrapolated to 1 M M^+, pH 7.0, 25 °C. [c] For fixed $n = 4$; pH 7.0, 25 °C. [d] For linearized pUC8 DNA, $n = 4$, pH 6.0, 25 °C (Mascotti & Lohman, 1993). [e] For sonicated calf thymus DNA, $n = 3.6-5.4$, pH 6.5, 25 °C (Braunlin et al., 1982). [f] Errors are estimated from the reported linear regression and errors on the slope and intercept.

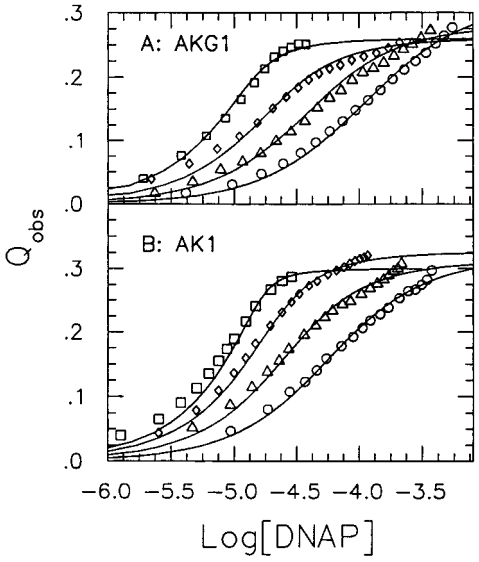

FIGURE 4: Representative reverse titrations of the helical oligopeptide, AK1, and nonhelical oligopeptide AKG1 with CT DNA at pH 7.0, 25 °C, and different [Na^+]. The observed fluorescence quenching (cf. eq 2) is plotted vs the logarithm of the molar concentration of DNA phosphate (monomer). (A) AK1 (initial oligopeptide concentrations of 3.1 μM). (B) AKG1 (initial oligopeptide concentrations of 2.23, 2.54, 3.18, and 3.18 μM, respectively) in 6.4 (□), 11.43 (◇), 16.46 (△), and 21.50 mM Na^+ (○). Solid lines are the best fittings using the McGhee−von Hippel isotherm (eq 3) with n fixed at its average value of ∼4 (cf. Table 4) and K_{obs} and Q_{max} floated.

Table 4. When all three parameters (K_{obs}, Q_{max}, and n) are floated, the resulting best-fit values of n are approximately 4 for each of the oligopeptides. Fittings of the data for fixed $n \gtrsim 5$ do not converge. The minor variations in the magnitude of n obtained from the global fittings exhibit no trend for compact (5-residue) vs extended (17-residue) oligopeptides. Values of n close to 4 also were obtained by an alternative approach, analyzing plots of Q_{obs} versus [DNAP]/[L_T] for AK1 and WK_4, which exhibit the largest values of K_{obs} of the oligopeptides we investigated. Consequently, to decrease the number of floated parameters, n was fixed at its average value of 4 in global fittings of reverse titration data with eq 3, which generated the smooth curves shown in Figures 3A−D. Values of Q_{max} and K_{obs} (Table 5) obtained with fixed $n = 4$ are similar to those listed in Table 4 with n floated.

In principle global fitting yields the best way of assessing how well a given nonlinear functional form can represent experimental data for a given set of conditions. However, the global fitting is not necessarily the best fitting for a single titration. In fact, the individual fitting (not shown) to each of the titrations is better than that obtained by global fitting with $n = 4$ (cf. Figure 3) and does eliminate the appearance of any systematic deviation between data points and the fitted curve. Binding constants obtained as averages from the individual fittings are not significantly different from those obtained by global fitting.

The maximum fluorescence quenching, Q_{max}, ranges from 0.26 ± 0.01 (AKG1) to 0.35 ± 0.01 (AK2) under the solution conditions investigated here and exhibits no systematic trend (cf. Table 4). Thus, the complexed states of these oligopeptides are inferred to be similar with regard to the environment of the N-terminal tryptophan. Values of Q_{max} for DNA-binding of all oligopeptides investigated here are significantly smaller than those observed for the binding of KWK_2 to linear or supercoiled pUC8 DNA (Q_{max}=0.47−0.50 at pH 6.0 in cacodylate buffer; Mascotti & Lohman, 1993). These differences in Q_{max} may reflect differences in the chemical environment of the interior tryptophan in KWK_2 from those of the terminal tryptophans in WK_4 and the extended AK or AKG oligopeptides (which, unlike KWK_2, are N-acetylated). For each of the oligopeptides in the present study the intrinsic fluorescence quantum yield of the N-terminal tryptophan is similar to that of free L-tryptophan, but higher than that of KWK_2 in the buffer used here (data not shown). The lower extents of tryptophan fluorescence quenching in the present study may also be due to the presence of buffer anions, such as phosphate, which can quench tryptophan fluorescence, as reported recently (Mascotti & Lohman, 1995). At [M^+] = 6.4 mM, K_{obs} is greater for AK1 than for AK2, AKG1, and AKG2, all of which are approximately the same. For all of the 17-residue oligopeptides, K_{obs} is almost an order of magnitude smaller than the value determined here for WK_4 and the values extrapolated to 6.4 mM M^+ for spermine (+4) (Braunlin et al., 1982) and KWK_2 (Mascotti & Lohman, 1992) (Table 5).

Dependence of K_{obs} on Salt Concentration. The dependence of K_{obs} on salt concentration was examined by using eq 3 to analyze fluorescence quenching data for two to three reverse titrations at each of four different M^+ concentrations in the range 6.4−21.5 mM. Over this range of [M^+], $f_{h,F}$, the fractional helicity of the free oligopeptide, does not change significantly (cf. Figure 2C). Representative plots of reverse titration data of oligopeptides for AK1 (helical) and for AKG1 (nonhelical) at similar initial bound oligopeptide concentrations are shown in Figures 4A and 4B, respectively. Some scatter in the data appears at the higher

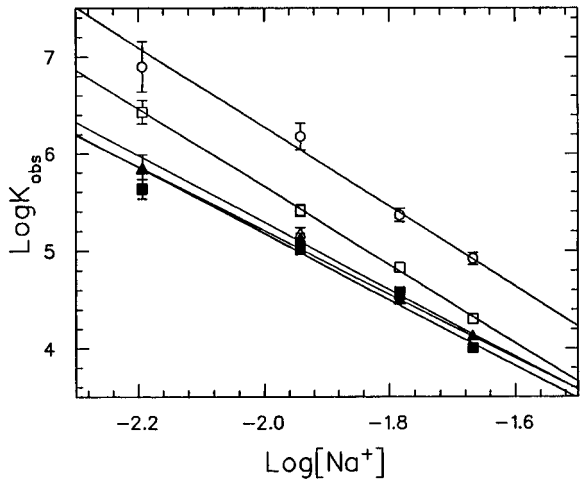

FIGURE 5: Plots of log K_{obs} vs log[Na^+] for the oligopeptides indicated (WK_4, ○; AK1, □; AK2, △; AKG2, ▲; AKG1, ■) at 25 °C, pH 7.0. K_{obs} at each salt concentration was obtained as described in the text. Lines represent linear least squares best fittings to the data (with parameters listed in Table 5).

Table 6: Energetics of Oligopeptide−DNA Binding and Coupled Conformational Changes (25 °C, pH 7.0, 6.4 mM M^+)

oligopeptide (L)	binding free energy[a] ΔG°_{obs} (kcal/mol)	cost of coupled conformational changes[b] $\Delta\mu_L^{conf}$ (kcal/mol)	cost of helix induction[c] $\Delta\mu_L^{MLR}$ (kcal/mol)
WK_4	−9.4 ± 0.3	0	0
AK1	−8.8 ± 0.2	+0.6 ± 0.5	0.4 ± 0.1
AK2	−8.0 ± 0.2	+1.4 ± 0.5	0.4 ± 0.1
AKG1	−7.7 ± 0.1	+1.7 ± 0.4	0.0 ± 0.1
AKG2	−7.9 ± 0.1	+1.5 ± 0.4	0

[a] Calculated for each oligopeptide from best-fitted value of K_{obs} using eq 3 with $n = 4$ (as in Table 5). [b] Calculated using eq 5. [c] Calculated using eq 4 (as in Table 3).

(fixed) values of [M^+] and/or [DNAP], probably because of the weaker binding of the oligopeptide and/or the relatively larger magnitude of corrections to the fluorescence signal. However, in all cases the quenching data are adequately described by eq 3. Fittings of these reverse titration data yield values of $n \cong 4$ when n is floated (data not shown) at each fixed [M^+]. For each oligopeptide Q_{max} does not vary with [M^+] outside experimental uncertainty. Values of log K_{obs} for all the oligopeptides decrease linearly with log[M^+] in the salt concentration range examined here and have similar slopes (SK_{obs}) ranging from -3.3 ± 0.1 to -4.1 ± 0.3, with an average value of -3.7 ± 0.4 (cf. Figure 5 and Table 5).

Effects of Coupled Conformational Changes of a Ligand on the Thermodynamics of Its DNA Binding. Values of K_{obs} for the binding of compact (+4) oligocations (WK_4, KWK_2, spermine) to double-stranded DNA at 6.4 mM M^+ are approximately 10^7 M^{-1}, 1−2 orders of magnitude higher than those for the 17-residue extended (+4) AK and AKG oligopeptides. Corresponding values of ΔG°_{obs}, listed in Table 6, exhibit significant differences that we propose are due to the costs of conformational changes that occur upon binding to DNA. The average value of n for the extended oligopeptides is 4 ± 0.5, the same within uncertainty as that of the compact oligopeptide WK_4. From this similarity in n, and the reduction in ΔG°_{obs} for the extended oligopeptides compared to WK4, we infer that upon binding to DNA they assume more compact conformations, with charge distributions similar to that of WK_4.

The increase in f_h observed by CD for AK1, AK2, and AKG1 when each is bound to DNA demonstrates that an increase in α-helical structure is one type of conformational change coupled to DNA binding (cf. Table 2). Other types of conformational changes also could be involved in producing the more compact bound states of some of these extended oligopeptides (e.g., AKG2). The thermodynamic effects of conformational changes accompanying oligopeptide−DNA binding are quantified by applying the following analysis.

As evaluated via eq 3 from the tryptophan fluorescence quenching data, the observed standard binding free energy ΔG°_{obs} is obtained from $\Delta G^\circ_{obs} \equiv -RT \ln K_{obs}$. Because the values of n and SK_{obs} that we have determined for each of the four extended oligopeptides are close to the corresponding values determined for WK_4, we assume that all contributions to ΔG°_{obs} other than those resulting from conformational changes are the same for each of the oligopeptides (extended and compact) investigated here. Therefore, ΔG°_{obs} for the binding to DNA of each of the extended oligopeptides is expressed as the sum of two terms:

$$\Delta G^\circ_{obs} = \Delta G^\circ_{obs,WK_4} + \Delta G^{conf} \quad (5)$$

Here $\Delta G^\circ_{obs,WK_4}$ is the binding free energy of a compact tetravalent ligand (WK_4), for which ΔG^{conf}, the conformational contribution, is zero, because binding-induced conformational changes are not expected in this compact oligopeptide.

For a binding equilibrium of the type considered here, the formation of the complex LD in general could produce changes in the conformations of both L and D. The observed increases in f_h for three of the extended oligopeptides are clear indications that binding to DNA induces additional α-helical structure in these ligands (as shown in Table 3). In agreement with previous studies of specific and nonspecific binding of oligopeptides to DNA (O'Neil et al., 1990, 1991; Talanian et al., 1990; Johnson et al., 1994), our spectroscopic results provide no indication of any change in the double-helical structure of the DNA itself upon binding of an oligopeptide ligand. Consequently, the conformational change accompanying the binding interaction in each of these systems is attributed entirely to a change in the excess chemical potential of the ligand, so that $\Delta G^{conf} = \Delta\mu_L^{conf}$, where μ_L^{conf} is the conformational contribution to the excess chemical potential of the oligopeptide (as defined in the Appendix).

The values of $\Delta\mu_L^{conf}$ listed in Table 6 were calculated with eq 5 from our experimental determinations of ΔG^{conf} for each of the extended oligopeptides. Because of the relatively large uncertainty in $\Delta G^\circ_{obs,WK_4}$, the error bars on our reported values of $\Delta\mu_L^{conf}$ generally overlap. Of course, pairwise comparisons of the DNA-binding energetics of different extended oligopeptides should be made in terms of ΔG°_{obs}, rather than $\Delta\mu_L^{conf}$, to avoid unnecessary compounding of experimental uncertainties. The purpose of estimating values of $\Delta\mu_L^{conf}$ with eq 5 is strictly to make comparisons with corresponding theoretical predictions.

If $\Delta\mu_L^{conf}$ were due entirely to the induction of α-helical structure when the oligopeptide binds to DNA, it could be estimated theoretically, using eq 4, by applying the modified

Lifson−Roig (MLR) model (explained in the Appendix) to analyze the observed change in f_h for bound and free oligopeptides. Values of $\Delta\mu_L^{MLR}$ calculated in this way are given in Table 6 for binding to DNA of each 17-residue oligopeptide at 25 °C and 6.4 mM Na^+, for comparison with the corresponding values of $\Delta\mu_L^{conf}$ estimated with eq 5. For AK1, $\Delta\mu_{AK1}^{conf}$ is approximately equal to $\Delta\mu_{AK1}^{MLR}$, the theoretical estimate of the free energy cost of additional induced α-helical structure. For each of the other extended oligopeptides, $\Delta\mu_L^{conf}$ is significantly larger than the corresponding value of $\Delta\mu_L^{MLR}$. Physical implications of these differences are discussed below.

DISCUSSION

Nonspecific DNA-Binding of Tetracationic Ligands (L^{4+}) of Diverse Types Exhibits Common Thermodynamic Characteristics. The DNA-binding of the tetracationic oligopeptides examined here [AK and AKG (both extended) and WK_4 (compact)] and previously [spermine (Braunlin et al., 1982) and KWK_2 (Mascotti & Lohman, 1993), both compact], show many striking similarities, even though these ligands differ from one another in number of residues, charge distribution, and primary and secondary structure and even though the extended oligopeptides exhibit a wide range of increases in fractional helicity upon binding to DNA. For all of the +4 ligands investigated here (as well as spermine and KWK_2), the binding to DNA is characterized by similar site sizes (average $n = 4 \pm 0.5$) and similar power dependences on $[M^+]$ (average $SK_{obs} = -3.7 \pm 0.4$). Both n and SK_{obs} are independent of salt concentration over the range investigated. All of the extended (17-residue) oligopeptides investigated in the present study exhibit a relatively narrow range of the observed binding constants K_{obs}, from approximately 4.3×10^5 to 2.7×10^6 M^{-1} at 6.4 mM M^+, which are 1−2 orders of magnitude smaller than K_{obs} for compact ligands having the same charge (+4) at the same $[M^+]$.

L^{4+} Ligands Exhibit Site Sizes of ∼4 in DNA Binding. Despite the significant differences in chain lengths (17 vs 5 amino acid residues) and in the increase in f_h induced upon binding to DNA, McGhee−von Hippel (1974) analyses of titrations of all the oligopeptides investigated here yield site sizes (n) of approximately 4 DNA phosphates. For nonspecific binding of *compact* oligocations, the approximate equality of n and z (the ligand charge) has been observed previously (McGhee & von Hippel, 1974; Record et al., 1976; Braunlin, 1982; Plum & Bloomfield, 1988; Mascotti & Lohman, 1992, 1993; Zhang et al., 1996). The analogous finding for extended oligocationic ligands is reported here for the first time.

In view of the correspondence of n and z for both extended and compact oligopeptides, we propose that differences in the values of ΔG°_{obs} determined here between the compact and any of the extended +4 oligopeptides, and among the latter, result from different extents and/or types of conformational changes that accompany binding to DNA. Our CD data demonstrate variable extents of induction of additional α-helical structure in the bound oligopeptides (except AKG2). The differences between $\Delta\mu_L^{conf}$ and $\Delta\mu_L^{MLR}$ (shown in Table 6 and considered in more detail below) imply the occurrence of conformational change(s) of some other type(s) when AK2, AKG1, and AKG2 bind to DNA.

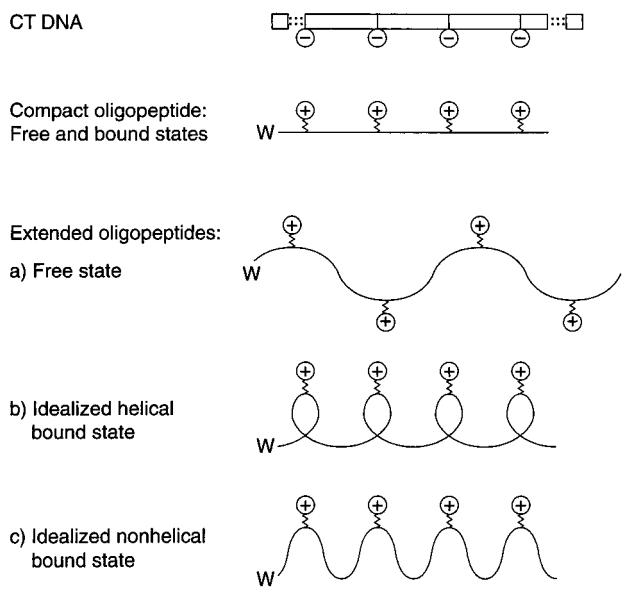

FIGURE 6: Schematic representation of the effects of different oligopeptide conformations on their binding interactions with ds DNA. DNA phosphate charges and lysine side-chain charges are represented in the circles with − and + signs, respectively.

For example, intervening uncharged residues in these extended oligopeptides may "loop out" upon binding to produce a relatively compact conformation as illustrated in Figure 6. The cost in free energy due to enhanced coulombic repulsions between lysine charges and the loss of entropy incurred by compaction of the oligopeptide conformation must be more than compensated by favorable coulombic interactions between lysine and DNA phosphate charges.

L^{4+} Ligands Exhibit Similar Power Dependences of K_{obs} on Salt Concentration. Values of K_{obs} for the DNA-binding of the extended AK and AKG peptides (all tetracationic but with differences in primary structure, charge distribution, and helicity in the bound and unbound states) show power dependences on salt concentration with similar values of SK_{obs} (averaging -3.7 ± 0.4 and ranging from −3.3 to −4.1). This minor variation in SK_{obs} could be due to variations in the salt-dependence of $\Delta\mu_L^{conf}$ for the different oligopeptides. However, under the conditions of the present study this effect is too close to experimental uncertainty to be analyzed quantitatively.

For the DNA binding of all the oligopeptide ligands that have been investigated here and elsewhere, SK_{obs} is found to be relatively insensitive to the details of initial ligand size, shape, and charge distribution. The values of SK_{obs} determined here for four extended oligopeptides are similar to those reported previously for the more compact ligands having the same net positive charge, such as spermine ($SK_{obs} = -3.3 \pm 0.3$; Braunlin et al., 1982), KWK_2 ($SK_{obs} = -3.5 \pm 0.3$; Mascotti & Lohman, 1993), and WK_4 ($SK_{obs} = 4.1 \pm 0.3$; this study). Results consistent with ours also were reported by Mascotti and Lohman (1992, 1993) for the binding interactions of single-stranded polynucleotides with three compact oligolysines having the same number of lysines (5) interspersed with one to three tryptophans. Values of SK_{obs} for binding of oligocationic ligands to DNA are the same in Na^+ and K^+ salts (Mascotti & Lohman, 1990). Values of K_{obs} extrapolated to $[M^+] = 1$ M (Table 5) are small and unfavorable, as observed for other primarily coulombic interactions of oligocations (L^{Z+}) with DNA

(Record et al., 1976; Braunlin et al., 1982; Plum & Bloomfield, 1988; Mascotti & Lohman, 1990, 1992; Zhang et al., 1996).

A detailed thermodynamic analysis of SK_{obs} for ligand−DNA binding has been formulated in terms of preferential interaction coefficients (Anderson & Record, 1993). On the basis of a standard simplified model for the ligand and the polyelectrolyte solution, SK_{obs} has been evaluated using the counterion condensation concept (Record et al., 1976, 1978; Manning, 1978), grand canonical Monte Carlo simulations (Olmsted et al., 1995), and the Poisson−Boltzmann (PB) equation (Zhang et al., 1996; Rouzina & Bloomfield, 1996). More structurally detailed models also have been used to evaluate SK_{obs} for specific binding of some cationic (+2) ligands and proteins via numerical solutions of the PB equation (Misra et al., 1994; Sharp, 1995). Theoretical calculations of SK_{obs}, for the DNA-binding of various ligands, ranging in complexity from compact oligocations to proteins, have been reviewed recently (Anderson & Record, 1995). These calculations, although based on model assumptions and approximations (fundamental and numerical) that differ in some important respects, all are predicated on the primary importance of coulombic interactions as determinants of SK_{obs}. This crucial assumption is supported further by the results of the present study. For oligocation-DNA binding, previous experimental work [cf. Zhang et al. (1996) and references therein] demonstrates that the magnitude of SK_{obs} is determined primarily by the thermodynamic effect of the release of accumulated cations that accompanies the reduction in polyanion DNA charge density when an oligocation binds.

For Binding of L^{4+} Ligands to Polyanionic DNA, the Magnitude of K_{obs} Is Correlated with Ligand Charge Density in the Unbound State. Values of K_{obs} (6.4 mM M^+, 25 °C) for all of the extended 17-residue AK and AKG oligopeptides differ by less than an order of magnitude (ranging from 4.3×10^5 to 2.7×10^6 M^{-1} for $n = 4$). The corresponding trend in ΔG°_{obs} is related to effects of conformational changes, as discussed in the following section. Here we consider comparisons between the binding energetics of the extended oligopeptides and three more compact tetracationic ligands of higher charge density (spermine, KWK_2, and WK_4). The compact +4 ligands exhibit values of K_{obs} (ranging from 7.9×10^6 to 2.7×10^7 M^{-1}) which are significantly higher than those of any of the extended oligopeptides. Because of the shorter chain lengths and the higher coulombic replusions among the lysine charges, KWK_2 and WK_4 are expected to have zero helicity whether bound to DNA or free in solution. Thus, tighter DNA-binding of each of these compact +4 oligocations could reflect their higher unbound charge density as well as the absence of any significant conformational change upon binding (cf. Figure 6). The correlation between higher DNA-binding affinity and higher charge density of the unbound ligand is consistent with several previous spectroscopic and thermodynamic studies of relative DNA-binding affinities of inorganic cations and (poly)amines of the same charge but different charge density: Na^+ vs $(CH_3)_4N^+$, Mg^{2+} vs putrescine (+2), and $Co(NH_2)_6^{3+}$ vs spermidine (+3) (Bleam et al., 1980; Braunlin et al., 1982, 1987; Padmanabhan et al., 1991).

Differences in ΔG°_{obs} for Binding to DNA of L^{4+} Ligands Can Be Attributed to Differences in Coupled Conformational Changes. The values of $\Delta\mu_L^{conf}$ listed in Table 6, as calculated by eq 5, are intended to contain all contributions of conformational changes in the ligand to the overall ΔG°_{obs} for a given ligand−DNA binding interaction. For binding to DNA of the extended oligopeptides AK and AKG, ΔG°_{obs} ranges from −7.7 to −8.8 kcal/mol, about 1.1−2.2 kcal/mol less favorable than the values for compact rigid tetravalent ligands ($\Delta G^\circ_{obs} = -9.9 \pm 0.3$ kcal/mol). The corresponding values of $\Delta\mu_L^{conf}$, estimated with eq 5 for each of the extended L^{4+} oligopeptide ligands, are no larger than the change in binding free energy that would result from decreasing the ligand charge by one unit. At the salt concentration investigated (6.4 mM M^+), the increase in the magnitude of DNA-binding free energy is ∼2 kcal/mol per added positive charge, as determined for the series putrescine (+2), spermidine (+3), spermine (+4) (Braunlin et al., 1982), and for KWK_2 (+4) vs KWK_4 (+6) binding to double-stranded (linear and circular) plasmid DNA (Mascotti & Lohman, 1992).

We infer from CD measurements that oligopeptide−DNA binding does not cause any conformational change in the 160 bp DNA but does induce additional α-helicity in AK1 and AKG1, both of which have two pairs of (*i*,*i*+4) spaced lysines. This inference is consistent with the observation reported by Johnson et al. (1994) that nonspecific binding to DNA induces increased fractional helicity in alanine−lysine oligopeptides that have (*i*,*i*+4) lysine spacing, which form amphipathic helices. We find additional helix induction also in bound AK2, with (*i*,*i*+5) lysine spacing, but not in bound AKG2. Johnson et al. (1994) found no additional helix induction upon binding to DNA of an oligopeptide similar to AK2 (except that the N-terminal tryptophan was replaced by a tyrosine). However, this result could stem from the weaker binding conditions examined (higher salt concentrations and shorter DNA).

The free energy cost associated with forming the more compact conformations of bound ligands diminishes the magnitudes of ΔG°_{obs} for the extended 17-residue oligopeptides from the values obtained for spermine, KWK_2, or WK_4. In AK1, the two (*i*,*i*+4) spacings between lysine residues permits placement of positive charges on the same side of the α-helix (nearly an amphipathic helix) and thereby could favor contacts between lysine charges and DNA phosphates. Accordingly, at 25 °C $\Delta\mu_{AK1}^{conf} = 0.4 \pm 0.5$ kcal/mol of peptide, which within experimental uncertainty does not differ from the theoretically calculated free energy cost of additional helix induction, $\Delta\mu_{AK1}^{MLR} = 0.4 \pm 0.1$ kcal/mol (Table 6). However, $\Delta\mu_{AK2}^{conf} = 1.4 \pm 0.5$ kcal/mol significantly exceeds $\Delta\mu_{AK2}^{MLR} = 0.4 \pm 0.1$ kcal/mol (Table 6). This difference indicates that, in addition to induction of the α-helical secondary structure, other significant conformational changes may occur (because of the different primary lysine spacing in AK2) to optimize favorable contacts between lysine charges and DNA phosphates. For the glycine-containing oligopeptides, $\Delta\mu_{AKG1}^{conf} = 1.7 \pm 0.5$ kcal/mol and $\Delta\mu_{AKG2}^{conf} = 1.4 \pm 0.5$ kcal/mol, respectively. In both cases the corresponding is significantly smaller in magnitude. The positive values of $(\Delta G^\circ_{obs,AKG} - \Delta G^\circ_{obs,AK1})$ reflect the greater disorder of the unbound states of the AKG oligopeptides (smaller f_h determined by CD measurements). Thus, compaction of the glycine-containing oligopeptides

upon binding to DNA entails a greater cost in conformational free energy.

The observed differences between $\Delta\mu_L^{conf}$ and $\Delta\mu_L^{MLR}$ imply that the MLR model does not suffice to describe all of the conformational changes in the oligopeptide L that occur upon binding to DNA. This inadequacy could arise, for example, if coil (nonhelical) states of certain residues are no longer energetically equivalent when the oligopeptide is bound to DNA. In this situation a matrix different from that used in the MLR model would be required to generate the ensemble of conformational states of the bound oligopeptide. Any more detailed statistical thermodynamic description of these conformational states could be reliably parametrized only on the basis of structural information that is not currently available.

All of our results are consistent with the following conclusions. Extended alanine/lysine/glycine oligopeptides, which may serve as models for DNA-binding regions of larger proteins, exhibit significant conformational changes, including α-helix formation, upon binding to DNA. Coulombic interactions of lysine charges with DNA phosphates reduce the DNA axial charge density and thereby drive the nonspecific DNA binding of these cationic ligands. Coupled conformational changes produce a compact state of the bound ligand that interacts more favorably with the DNA phosphates (as illustrated by examples shown in Figure 6). As a result of this compaction the magnitudes of ΔG°_{obs} are reduced for the DNA binding of extended oligopeptides, in comparison to the compact oligopeptide WK_4 having the same charge.

ACKNOWLEDGMENT

We thank Drs. R. L. Baldwin, T. M. Lohman, P. S. Kim, and R. S. Saecker for helpful discussions and/or for their valuable comments on the manuscript and Dr. Baldwin for access to the AVIV 60DS CD spectropolarimeter and the programs (originally written by J. A. Schellman) implementing the modified Lifson−Roig model of helix−coil transition. We also thank Drs. P. H. von Hippel and N. Johnson for a preprint of their paper and their comments on this manuscript and Drs. L. Smith and M. Fitzgerald for mass spectrometric measurements, C. Rohl for helpful discussion about aspects of the helix−coil transition and for providing the computer program to analyze CD data, and S. Aiello for her help in preparing the manuscript.

APPENDIX

Application of the Modified Lifson−Roig Model To Calculate the Conformational Contribution to the Change in Excess Chemical Potential of an Oligopeptide Accompanying Its Binding to Native DNA

Whether bound to DNA or free in solution, the relatively short oligopeptide chains investigated here do not have totally α-helical conformations. Under given conditions, the overall average "fractional helicity" of each oligopeptide, expressed as f_h (eq 1), was evaluated from CD measurements (as explained in Materials and Methods). Binding to DNA produces an increase in f_h for three of the four 17-residue oligopeptides under all of the conditions investigated in the present study. These changes in f_h reflect a coupling of the binding process to a change in the overall conformational state that includes, but may not be limited to, an increase in the α-helicity of the bound oligopeptide. The binding isotherms (as determined by the fluorescence spectroscopic method described in Materials and Methods) yield no indication of more than one class of bound oligopeptides. Consequently, a thermodynamic analysis of the contribution to the binding energetics that is due to a conformational change of the oligopeptide can be based on a two-state picture, taking into account only the average α-helicity (or, more generally, average conformation) of an oligopeptide that is either bound to DNA or free. The difference in free energy between the bound and free states can be described theoretically as due to a shift in the populations of all possible (i.e., sterically allowed) conformational states of the oligopeptide chain. In our implementation of statistical thermodynamic calculations of the change in free energy due to a shift in the average oligopeptide conformation, no *a priori* assumptions are made about the extent of fractional helicity of oligopeptides in either the bound or the free state.

In general the conformation of an oligopeptide depends on temperature, salt concentration, and the presence of other species (e.g., DNA) to which it can bind. At the molecular level the orientations of individual bond angles along the oligopeptide chain are determined not only by relatively local intramolecular interactions, such as hydrogen bonds, but also by coulombic interactions with charges on the oligopeptide, on DNA, and/or on salt ions in solution. The ensemble of conformations of an oligopeptide can be enumerated and appropriately weighted by constructing a conformational partition function, Z^{conf}. Because this partition function is of the "semigrand" type, as discussed for example by Schellman (1975), the conformational contribution to the excess chemical potential of the oligopeptide can be expressed as $\mu^{conf} = -RT \ln Z^{conf}$. [The relevance of Z^{conf} in this context was suggested to us by C. Rohl (private communication).] If binding to polyanionic ds-DNA is accompanied by a shift in the population of the conformational states of a ligand L, then the corresponding change in $\Delta\mu_L^{conf}$, the conformational part of the excess chemical potential of L, can be expressed as

$$\Delta\mu_L^{conf} = RT \ln(Z_B^{conf}/Z_F^{conf}) \qquad \text{(A1)}$$

Here B and F denote the bound and free states of L, respectively.

For a given set of solution conditions, the magnitude of $\Delta\mu_L^{conf}$ is determined, in general, by differences in the thermodynamic effects of both coulombic and noncoulombic interactions on the conformation of L in the bound and free states. In addition to $\Delta\mu_L^{conf}$, various other types of contributions determine the values of ΔG°_{obs} obtained here by analysis of fluorescence quenching data for the oligopeptide−DNA binding process. In general, intermolecular and intramolecular effects of both coulombic and noncoulombic interactions contribute to the magnitude of ΔG°_{obs}, which also depends in an obvious way on the units chosen to express the concentrations of reactants and products in the stoichiometric equilibrium quotient, K_{obs}. Under the conditions of interest here (typical of most in vitro studies) the only composition variable that determines the magnitude of ΔG°_{obs} at fixed T and P is the concentration of excess salt.

If the only significant conformational change that accompanies oligopeptide−DNA binding can be monitored by

using CD measurements to determine the change in f_h of the oligopeptide, Z_L^{conf} can be evaluated theoretically using the modified Lifson−Roig (MLR) model (Lifson & Roig, 1961; Qian & Schellman, 1992; Doig et al., 1994). In calculating Z_L^{MLR}, the oligopeptide is modeled as a chain of "residues", each of which may be in either of only two conformational states. Specifically, a residue corresponds to the α-carbon attached to a peptide unit in the chain (defined by the MLR model to include both N-acetylated and C-amidated termini). The conformational state of each residue is designated "**h**" or "**c**" solely on the basis of the torsional angles ϕ and ψ formed by bonds attached directly to the α-carbon. Then each possible conformation of the oligopeptide chain can be represented as a linear array of sequences of consecutive **h** or **c** residues. For steric reasons, any α-helical stretch must contain at least three consecutive **h** residues so that at least one H-bond can be formed. Accordingly, isolated **h** residues can appear, singly or as an adjacent pair, in stretches of the oligopeptide chain that are not α-helical, although no **c** residue ever appears in an α-helical stretch.

In constructing Z_L^{MLR} for an oligopeptide chain, each of the two residue states is assigned one of several different types of statistical weights, selected according to the conformational state of adjacent residues. With the appropriate set of statistical weights as the only input, Z_L^{MLR} can be evaluated for an oligopeptide chain of N_r residues by direct matrix multiplication, which we implemented with a program originally written by John Schellman [cf. Doig et al. (1994)]. A more detailed explanation of the four types of statistical weights that we used to construct Z_L^{MLR} for both bound and free states of each oligopeptide can be found in Doig et al. (1994). Here we adopt the assumption that any dependence of Z_L^{MLR} on temperature or solution composition can be attributed entirely to the statistical weight w, defined such that $-RT \ln w$ is the difference in free energy between an **h** residue located in an α-helical stretch and a **c** residue. In general w depends not only on solution conditions but also on various other factors, including the chemical nature of the groups attached to the α-carbon (Baldwin, 1995, and references therein). For the present calculations, the same average value of w was assigned to each type of helical peptide unit (alanine, lysine, glycine, tryptophan) in a given oligopeptide, because we require only the net thermodynamic effect on ΔG°_{obs} that arises from the shift in the average oligopeptide conformational state when it binds to DNA.

Because w is defined as a relative statistical weight, any difference between w_B and w_F contains information about effects of binding to DNA on both the **h** and the **c** states of a residue (provided that, as assumed in the MLR model, all sterically allowed nonhelical states are equivalent in free energy). Accordingly, we assume that Z_B^{MLR} differs from Z_F^{MLR} only because $w_B \neq w_F$. All other statistical weights that are needed to generate the ensemble of conformational states of the oligopeptide chain are taken to be unaffected when it binds to DNA. (The values assigned to these weights are listed in Materials and Methods.) To match a theoretical evaluation of Z_J^{MLR} (J = B, F) with a given experimental determination of f_{hJ}, a binary search algorithm (Chakrabartty, et al., 1994) was used to determine the value of w_J, and hence of Z_J^{MLR}, that satisfies the following equation, which has been discussed for example by Qian and Schellman (1992):

$$f_{h,J} N_r = \partial \ln Z_J^{MLR} / \partial \ln w_J \qquad \text{(A2)}$$

The (effective) numerical integration of this equation was accomplished via computer program (Doig et al., 1994), subject to the aforementioned constraints on all statistical weights other than w_J. After applying this approach to evaluate both Z_B^{MLR} and Z_F^{MLR} for a given oligopeptide under a given set of conditions, the values of $\Delta\mu_L^{MLR}$ listed in Table 6 were calculated on the basis of eq A1.

REFERENCES

Allen, F. S., Gray, D. M., Roberts, G. P., & Tinoco, I. J. (1972) *Biopolymers 11*, 853−879.

Anderson, C. F., & Record, M. T. Jr. (1983) In *Structure and Dynamics: Nucleic Acids and Proteins* Clementi, E., & Sarma, R., Eds.) pp 301−319, Adenine Press, New York.

Anderson, C. F., & Record, M. T., Jr. (1993) *J. Phys. Chem. 97*, 7116−7126.

Anderson, C. F., & Record, M. T., Jr. (1995) *Annu. Rev. Phys. Chem.* 46, 657−700.

Arrowsmith, C. H., Pachter, R., Altman, R. B., Lyer, S. B., & Jardetzky, O. (1990) *Biochemistry 29*, 6332−6341.

Baldwin, R. L. (1995) *Biophys. Chem. 55*, 127−135.

Bleam, M. L., Anderson, C. F., & Record, M. T., Jr. (1980) *Proc. Natl. Acad. Sci. U.S.A. 77*, 3085−3089.

Braunlin, W. H., Strick, W. H., & Record, M. T., Jr. (1982) *Biopolymers 21*, 1301−1314.

Braunlin, W. H., Anderson, C. F., & Record, M. T., Jr. (1987) *Biochemistry 26*, 7724−7731.

Chakrabartty, A., Kortemme, T., Padmanabhan, S., & Baldwin, R. L. (1993) *Biochemistry 32*, 5560−5565.

Chakrabartty, A., Kortemme, T., & Baldwin, R. L. (1994) *Protein Sci. 3*, 843−852.

Chan, S. C., Breslauer, K. J., Hogan, M. E., Kessler, D. J., Austin, R. H., Ojemann, J., Passner, J. M., & Wiles, N. C. (1990) *Biochemistry 29*, 6161−6171.

Chen, G. C., & Yang, J. T. (1977) *Anal. Lett. 10*, 1195−1207.

Doig, A. J., & Baldwin, R. L. (1995) *Protein Sci. 4*, 1325−1336.

Doig, A. J., Chakrabartty, A., & Baldwin, R. L. (1994) *Biochemistry 33*, 3396−3403.

Edelhoch, H. (1967) *Biochemistry 6*, 1948−1954.

Holzwarth, G., & Doty, P. (1965) *J. Am. Chem. Soc. 87*, 218−228.

Houghten, R. A. (1985) *Proc. Natl. Acad. Sci. U.S.A. 82*, 5131−5135.

Houghten, R. A., Degraw, S. T., Bray, M. K., Hoffman, S. R., & Frizell, N. D. (1986) *BioTechniques 4*, 522−528.

Jen-Jacobson, L., Lesser, D., & Kurpiewski, M. (1986) *Cell* 45, 619−629.

Johnson, M. L., & Frasier, S. G. (1985) *Methods Enzymol. 117*, 301−342.

Johnson, N. P., Lindstrom, J., Baase, W. A., & von Hippel, P. H. (1994) *Proc. Natl. Acad. Sci. U.S.A. 91*, 4840−4845.

Latt, S. A., & Sober, H. A. (1967a) *Biochemistry 6*, 3293−3306.

Latt, S. A., & Sober, H. A. (1967b) *Biochemistry 6*, 3307−3314.

Lewis, M., Chang, G., Horton, N. C., Kercher, M. A., Pace, H. C., Schumacher, M. A., Brennan, R. G., & Lu, P. (1996) *Science* 271, 1247−1254.

Lifson, S., & Roig, A. (1961) *J. Chem. Phys. 34*, 1963−1974.

Lohman, T. M., & Mascotti, D. P. (1992) *Methods Enzymol. 212*, 424−458.

Lohman, T. M., deHaseth, P. L., & Record, M. T., Jr. (1980) *Biochemistry 19*, 3522−3530.

Manning, G. S. (1978) *Q. Rev. Biophys.* 11, 179−246.

Marqusee, S., & Baldwin, R. L. (1987) *Proc. Natl. Acad. Sci. U.S.A. 84*, 8898−8902.

Mascotti, D. P., & Lohman, T. M. (1990) *Proc. Nat. Acad. Sci. U.S.A. 87*, 3142−3146.

Mascotti, D. P., & Lohman, T. M. (1992) *Biochemistry 31*, 8932−8946.
Mascotti, D. P., & Lohman, T. M. (1993) *Biochemistry 32*, 10568−10579.
Mascotti, D. P., & Lohman, T. M. (1995) *Biochemistry 34*, 2908−2915.
McClarin, J. A., Frederick, C. A., Wang, B.-C., Greene, P., Boyer, H. W., Grable, J., & Rosenberg, J. M. (1986) *Science* 234, 1526−1541.
McGhee, J. D., & von Hippel, P. H. (1974) *J. Mol. Biol. 86*, 469−489.
Misra, V. K. , Sharp, K. A., Friedman, R. A., & Honig, B. (1994) *J. Mol. Biol.* 238, 245−263.
Nelson, J. W., & Kallenbach, N. R. (1986) *Proteins 1*, 211−217.
Newman, M., Strzelecka, T., Dorner, L. F., Schildkraut, I., & Aggarwal, A. (1995) *Science 269*, 656−663.
Olmsted, M. C., Anderson, C. F., & Record, M. T., Jr. (1989) *Proc. Natl. Acad. Sci. U.S.A. 86*, 7766−7770.
Olmsted, M. C., Bond, J. P., Anderson, C. F., & Record, M. T., Jr. (1995) *Biophys. J. 68*, 634−647.
O'Neil, K. T., Hoess, R. H., & DeGrado, W. F. (1990) *Science 249*, 774−778.
O'Neil, K. T., Shuman, J. D., Ampe, C., & DeGrado, W. F. (1991) *Biochemistry 30*, 9030−9034.
Padmanabhan, S., Marqusee, S., Ridgeway, T., Laue, T. M., & Baldwin, R. L. (1990) *Nature 344*, 268−270.
Padmanabhan, S., Brushaber, V. M., Anderson, C. F., & Record, M. T., Jr. (1991) *Biochemistry 30*, 7550−7559.
Percipalle, P., Simonscits, A., Zakhariev, S., Guarnaccia, C., Sanchez, R., & Pongor, S. (1995) *EMBO J. 14*, 3200−3205.
Plum, G. E., & Bloomfield, V. A. (1988) *Biopolymers 27*, 1045−1051.
Qian, H., & Schellman, J. A. (1992) *J. Phys. Chem. 96*, 3987−3994.
Record, M. T., Jr., & Anderson, C. F. (1995) *Biophys. J. 68*, 786−794.
Record, M. T., Jr., Lohman, T. M., & de Haseth, P. (1976) *J. Mol. Biol. 107*, 145−158.
Record, M. T., Jr., Anderson, C. F., & Lohman, T. M. (1978) *Q. Rev. Biophys. 11*, 103−178.
Record, M. T., Jr., Ha, J.-H., & Fisher, M. A. (1991) *Methods Enzymol.* 208, 291−343.
Rouzina, I., & Bloomfield, V. A. (1996) *J. Phys. Chem. 100*, 4292−4304.
Schellman, J. A. (1975) *Biopolymers 14*, 999−1018.
Scholtz, J. M., Qian, H., York, E. J., Stewart, J. M., & Baldwin, R. L. (1991a) *Biopolymers 31*, 1463−1470.
Scholtz, J. M., Marqusee, S., Baldwin, R. L., York, E. J., Stewart, J. M., Santoro, M., & Bolen, W. (1991b) *Proc. Natl. Acad. Sci. U.S.A. 88*, 2854−2858.
Scholtz, J., M., York, E. J., Stewart, J. M., & Baldwin, R. L. (1991c) *J. Am. Chem. Soc. 113*, 5103−5104.
Sharp, K. A. (1995) *Biopolymers* 36, 227−243.
Spolar, R. S., & Record, M. T., Jr. (1994) *Science 263*, 777−784.
Stein, V. M., Bond, J. P., Capp, M. W., Anderson, C. F., & Record, M. T., Jr. (1995) *Biophys. J. 68*, 1063−1072.
Talanian, R. V., McKnight, C. J., & Kim, P. S. (1990) *Science 249*, 769−771.
Wang, L., Ferrari, M., & Bloomfield, V. A. (1990) *BioTechniques 9*, 24−27.
Zhang, H., Zhao, D., Revington, M., Lee, W., Jia, X., Arrowsmith, C., & Jardetzky, O. (1994) *J. Mol. Biol. 238*, 592−614.
Zhang, W., Bond, J. P., Anderson, C. F., Lohman, T. M., & Record, M. T., Jr. (1996) *Proc. Natl. Acad. Sci. U.S.A. 93*, 2511−2516.

BI962927A